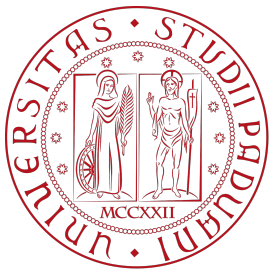

UNIVERSITÀ DEGLI STUDI DI PADOVA

Dipartimento di Fisica e Astronomia "Galileo Galilei"

Corso di Laurea in Fisica

Tesi di Laurea

Characterization of the kinematics of the rare decay $B_s \to \tau\tau$ with the CMS detector

Relatore

Prof. Tommaso Dorigo

Correlatore

Dr. Hevjin Yarar

Laureando

Alessandro Breccia

Anno Accademico 2021/2022

Abstract

This thesis present the results of the analysis of the kinematics relative to the decay of the B_s meson into a pair of τ leptons, made through the creation of high level features, aimed to be used in a signal vs background classification task by a Deep Neural Network. The frequency of this decay, never observed until now, is considered a sensitive variable for new physics beyond the Standard Model.

Contents

Chapter 1

Introduction

1.1 Rare decays in the Standard Model

All matter around us is made of elementary particles, the building blocks of matter. These particles are divided in two basic types called quarks and leptons. Each group consists of six particles, which are related in pairs, or "generations". Most of the stable matter in the universe is made from particles that belong to the first generation, the lightest one, any heavier particles quickly decay to more stable ones. The six quarks are grouped in three generations – the "up quark" and the "down quark" compose the first generation, the second generation is made by the "charm quark" and "strange quark", and the third generation is composed by "top quark" and "bottom (or beauty) quark". Quarks carries also a so-called "colour", which is the strong interaction charge, and only mix in such ways as to form colourless objects. The six leptons are similarly ordered in three generations – the "electron" and the "electron neutrino", the "muon" and the "muon neutrino", and the "tau" and the "tau neutrino". The electron, the muon and the tau all have an electric charge and a sizeable mass, whereas the neutrinos are electrically neutral and have very little mass.

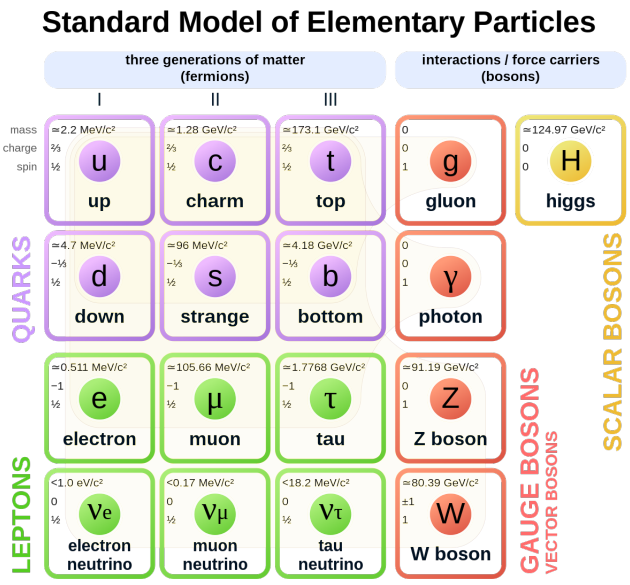

Figure 1.1: Standard Model of Elementary Particles Table

Moreover, there are four fundamental forces at work in the universe: the strong force (S.I.), the weak force (W.I.), the electromagnetic force (E.M.), and the gravitational force (G). They have

different strengths($G < W.I. < E.M. < S.I.$) and different ranges (∞ for G and E.M.; really short and dominant only at subatomic levels for W.I and S.I.). Three of the fundamental forces result from the exchange of force-carrier particles, which belong to a broader group called bosons. The latter are responsible of energy exchanges between particles of matter. Each fundamental force has its own corresponding boson: the strong force is carried by the gluon, the electromagnetic force is carried by the photon, and the W and Z bosons are responsible for the weak force. Following this line, the graviton should be the corresponding force-carrying particle of gravity, however it has not yet been found.
Even though the Standard Model is currently the best description of the subatomic world, it does not explain the complete picture of physics. The theory incorporates only three out of the four fundamental forces, omitting gravity. There are also important questions that it does not answer, such as "What is dark matter?", or "What happened to the antimatter after the big bang?"[1]. So although the Standard Model accurately describes the phenomena within its domain, it is still incomplete and do not suits the so-called "naturalness"[2].

1.2 The B_s meson in the SM

Processes where a B meson decays into a pair of oppositely charged leptons are powerful probes in the search for physics beyond the Standard Model (SM).The observation of the $B_s^0 \to \mu^+\mu^-$ decay has made possible the analysis of its branching fraction (B), which is compatible with the SM prediction and imposes stringent constraints on theories beyond the model. Complementing this result with searches for the tauonic modes $B \to \tau^+\tau^-$ (B^0 or a B_s^0) is of great interest in view of the recent hints of lepton flavour non-universality obtained by several experiments. In particular the measurements of $R\left(D^{(*)}\right) = \frac{\mathcal{B}\left(B^0 \to D^{(*)}\tau^+\nu_\tau\right)}{\mathcal{B}\left(B^0 \to D^{(*)}\ell^+\nu_\ell\right)}$,where l^+ stands for lepton, are found to be larger than the SM prediction by 3.9 standard deviations, and $R_K = \frac{\mathcal{B}\left(B^+ \to K^+\mu^+\mu^-\right)}{\mathcal{B}(B^+ \to K^+e^+e^-)}$ is 2.6 standard deviations lower than SM prediction[3]. Possible explanations for these and other deviations from their SM expectations include leptoquarks[4]-[5], W'/Z' bosons and other new theories, in which the $B \to \tau\ \tau$ branching fractions could be enhanced with respect to the SM predictions $\mathcal{B}\left(B^0 \to \tau^+\tau^-\right) = (2.22 \pm 0.19) \times 10^{-8}$ and $\mathcal{B}\left(B_s^0 \to \tau^+\tau^-\right) = (7.73 \pm 0.49) \times 10^{-7}$[6], by several orders of magnitude.
However, tau leptons reconstruction is quite complex at LHC, due to the their frequent hadron decays, and this signature is hidden by huge QCD backgrounds.

τ **Decay Modes**		
	Mode	**Fraction** Γ_i/Γ
Γ_1	$particle^- \geq 0 neutrals \geq 0 K^0 \nu_\tau$ ("1-prong")	$(85.24 \pm 0.06)\%$
Γ_2	$particle^- \geq 0 neutrals \geq 0 K_L^0 \nu_\tau$	$(84.58 \pm 0.06)\%$
Γ_{62}	$h^- h^- h^+ \geq 0 neutrals \geq 0 K_L^0 \nu_\tau$	$(15.20 \pm 0.06)\%$
Γ_{63}	$h^- h^- h^+ \geq 0 neutrals \nu_\tau (ex. K_S^0 \to \pi^+\pi^-)$ ("3-prong")	$(14.55 \pm 0.06)\%$
Γ_{64}	$h^- h^- h^+ \nu_\tau$	$(9.80 \pm 0.05)\%$

Figure 1.2: Tau hadron decay modes with relative branching fractions, from PDGlive [7]. "$h^\pm$" stands for $\pi^\pm$ or $K^\pm$, "neutrals" stands for γ's and/or π^0's

Moreover, selecting the $B_s \to \tau\tau$ signal represents a hard challenge at triggering level, so we rely on the μ only. Next we need a identifiable signal: in order to do that, we rely on one lepton: the $\tau \to \mu\bar{\nu_\mu}\nu_\tau$ decay has a small branching fraction, therefore for the other τ we ask for an hadronic decay recognizable from the noise background, and chosen one is the so-called "3-prong" decay, with the signature made up of the production of 3 π's.

To go deeper in the chain details, one τ lepton is reconstructed through the decay $\tau \to$

$\pi^-\pi^+\pi^-\nu_\tau$, with a branching fraction $\mathcal{B}(\tau \to \pi^-\pi^+\pi^-\nu_\tau) = (9.31\pm0.05)\%$, which proceeds predominantly through the decay chain $\tau \to a1(1260)^-\nu_\tau$, $a1(1260)^- \to \rho(770)^0\pi^-$. The remaining τ of the couple decays β into a μ and 2 neutrinos (ν_τ and $\bar{\nu_\mu}$), through a weak interaction mediated by the W^-, as in the other branch of the decay chain. The experimental search for $B_s \to \tau\ \tau$ decays is complicated also by the presence of at least two undetected neutrinos, originating from the τ decay. For the B^0 we have information from the BaBar collaboration, which has searched for the $B^0 \to \tau\ \tau$ mode[8], and published an upper limit $\mathcal{B}\,(B^0 \to \tau^+\tau^-) < 4.10\times10^{-3}$ at 90% confidence level (CL).

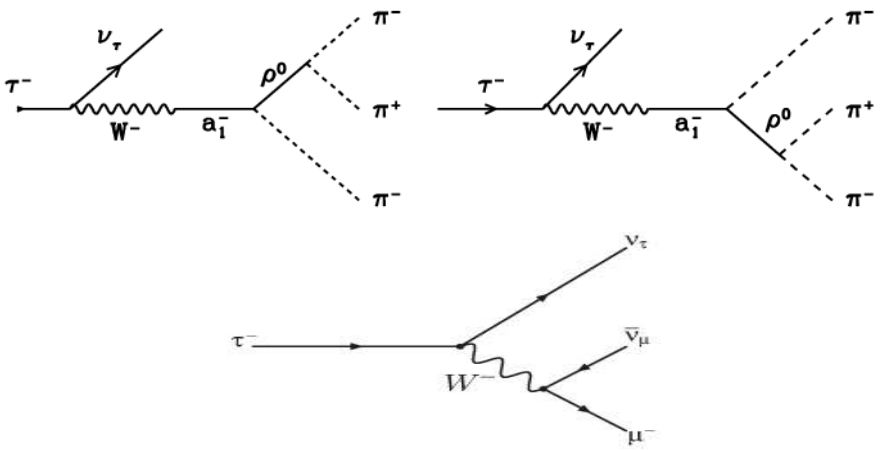

Figure 1.3: Tau decays involved in the $B_s \to \tau\ \tau$ process[9]

Chapter 2

The experimental apparatus

2.1 LHC

The Large Hadron Collider (LHC) is the world's largest and most powerful particle accelerator. It first started up on 10 September 2008, and remains the latest addition to CERN's accelerator complex[10]. The LHC consists of a 27-kilometre ring of superconducting magnets with series of accelerating structures to boost the energy of the particles along the way. Inside the accelerator, two high-energy particle beams travel at close to the speed of light before they are made to collide. The beams travel in opposite directions in separate beam pipes – two tubes kept at ultrahigh vacuum. They are guided around the accelerator ring by a strong magnetic field maintained by superconducting electromagnets. This requires cooling the magnets to -271.3°C – a temperature colder than outer space. For this reason, the magnets are connected to a distribution system of liquid helium, which cools the magnets. From the CERN Control Centre the beams inside the LHC are made to collide at four locations around the accelerator ring, corresponding to the positions of four particle detectors – ATLAS, CMS, ALICE and LHCb.

2.2 CMS Detector

The Compact Muon Solenoid (CMS) is a general-purpose detector at the Large Hadron Collider (LHC). It has a wide physics programme ranging from studying the Standard Model (including the Higgs boson) to searching for extra dimensions and dark matter[11]. The CMS detector is built around a huge solenoid magnet. This takes the form of a cylindrical coil of superconducting cable that generates a field of 3.8 tesla. The field is confined by a steel "yoke" that forms the bulk of the detector's 14,000-tonne weight. The complete detector is 21 metres long, 15 metres wide and 15 metres high. It has, starting from the center of it, series of pixels and strips, that are trackers with high resolution, meant to reconstruct the particle track. The second layer is the Electromagnetic Calorimeter (ECAL), design to measure with high accuracy the energy of electron and photons: it consist in 76000 scintillating cristals ($PbWO_4$), with 25 χ_0 (radiation length). On top of it we have the Hadronic Calorimeter (HCAL), for the measurement of hadrons' energy, which consist of layers of dense material interleaved with tiles of plastic scintillators. Externally to the HCAL is located the solenoid magnet, essential to bend the path of charged particles, which provides a 3.8 Tesla axial field. The last section is constituted by muon detectors and return yoke: as the name CMS suggest, the main task of the detectors is revealing muons, using the muon barrels, while the return yoke aim is to shield the μ detection areas from other particles coming from inside, as well as closing the magnetic field lines of the inner solenoid, thus providing extra-bending power and helps the determination of muon momenta.

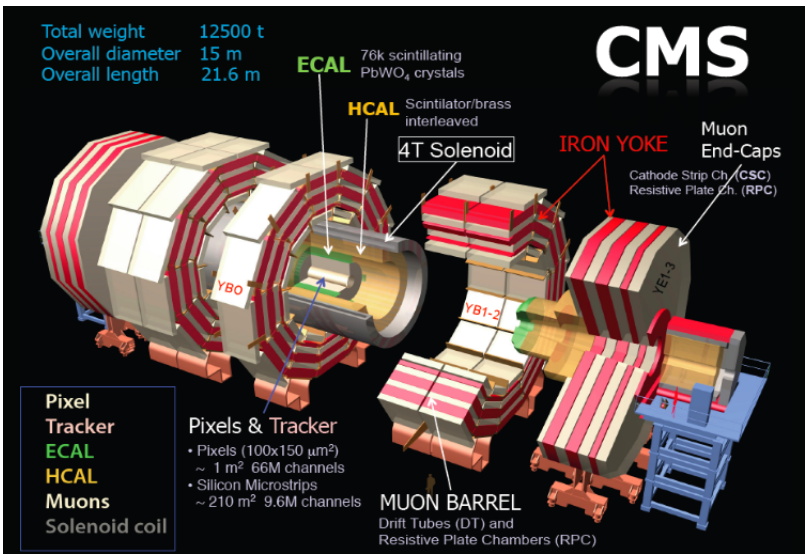

Figure 2.1: The Compact Muon Solenoid detector

2.3 Triggers

When CMS runs at its highest luminosity, about one billion proton-proton interactions will take place every second inside the detector. There is no possible way that data from all these events could be read out, and even in case it could, most would be hardly likely to reveal new phenomena. We hence need a "trigger" that can select the possibly interesting events, such as those which will produce a B_s meson, and reduce the rate to just a few hundred "events" per second, which can be read out and stored on computer disk for further analysis. However, with groups of protons colliding 40 million times per second, we have only 25 nanoseconds before the arrival of the next bunch. The solution is to store the data in pipelines that can temporarily store information from many interactions, allowing for their processing and selection at the same time. To not confuse particles from two different events, the detectors must have very good time resolution and the signals from the millions of electronic channels must be synchronised so that they can all be identified as being from the same event.

2.3.1 Triggering Levels

Level 1 of the trigger is an extremely fast and completely automatic process that looks for simple structures of interesting physics, e.g. particles with high energy levels or in unusual combinations. This is like a reader simply scanning the headlines of a newspaper to see if anything catches their eye[12]. Using this procedure we select the best 100,000 events or "issues" each second from the billion available.
For the next test, the higher level trigger, we assimilate and synchronise information from different parts of the detector to recreate the entire event - like collating the different pages to form the full newspaper - and send it to a cluster of more than 1000 standard computers. Here the PCs are like speed readers, who with more detailed information review the information for longer, less than a tenth of a second. They run very complex physics tests to look for specific signatures, for instance matching tracks to hits in the muon chambers, or spotting photons through their high energy but lack of charge.
Comprehensively a few hundred events per second are selected and the remaining ones are discarded. We are left with only the collision events from which we can learn something new about physics. Despite the trigger system, CMS still records and analyses several petabytes of data, that's millions of gigabytes, although not all these data are stored, usually. That was not the case of the B physics parking dataset: the BPHParked was designed with a simple goal,

which is record $\sim 10^{10}$ unbiased B hadron events during 2018 Run 2, to offer a unique test of the B physics flavor anomalies. Knowing that the DAQ capabilities go beyond the computing capacity of the experiment, the concept was to write on tape amount of data than normally, and "park"-it, so we could reconstruct them later during the LHC downtime. Trigger strategy has been carefully optimized to maximize the number of B hadrons to tape, given the fixed bandwidth. As of today, we have written to tape around 10^{10} events with approximately 70% purity.

Chapter 3

The data

3.1 B Physics Parking Dataset (BPHParked)

The B physics parking proposal was submitted to the CMS management in February 2018, with the main goal to make CMS competitive with LHCb in the $\frac{R(K)}{R(K^*)}$ measurements, which attracted a lot of attention in the last few years[13]. It also has potential to enable a number of new measurements in B physics sector, which were not possible before. The goal, as mentioned before, was to record $\sim 10^{10}$ unbiased B hadron events this year using the flexibility of the CMS data taking model. It was soon realized that the sample lends itself to a significantly broader program with a potential to revolutionize the way we do B physics in CMS. The number of B's we propose to put on tape rivals the full Run 1 event count of LHCb and offers a possibility of opposite-side tagging for time-dependent/CP-violation analyses. This project could profit from the key features of the CMS detector (excellent tracking, muon system, ECAL, τ ID) and make it competitive compared to LHCb on a number of important measurements of rare decays and searches for new states.

3.2 MonteCarlo Sample (MC)

Understanding the ultimate states of high energy particle collisions such as those at the Large Hadron Collider (LHC) is an extremely challenging theoretical problem. In a common collision, hundreds of particles are produced, and in most processes of interest their momenta extend over many orders of magnitude. All the particle species of the Standard Model (SM), and maybe some beyond, are involved so that the relevant matrix elements are too laborious to compute above the first few orders of perturbation theory, and in the case of QCD processes they involve the intrinsically non-perturbative and unsolved problem of confinement[14]. Once these matrix elements have been computed within some approximation methods, there remains the problem of facing with their many divergences and/or near-divergences. Finally they must be integrated over a final-state phase space of huge and variable dimension, obtaining predictions of experimental observables. Putting all these elements together, one has a Monte Carlo event generator capable of simulating a wide range of the most interesting processes that are expected at the LHC, which can be useful for several distinct purposes in HEP experiments. Event generators are usually required to extract a signal of new physics from the background of SM processes. Comparisons of their predictions to the data can be used to perform measurements of SM parameters. They also provide realistic input for the design of new experiments, or for new selection or reconstruction procedures within an existing experiment. The main MC generation software are *Pythia*, which is currently written in *C++*, as well as *Geant4*, one of the other common MC generation platform.

$$\sigma = \sum_{a,b} \int_0^1 \mathrm{d}x_a \, \mathrm{d}x_b \int f_a^{h_1}(x_a, \mu_F) \, f_b^{h_2}(x_b, \mu_F) \, \mathrm{d}\hat{\sigma}_{ab\to n}(\mu_F, \mu_R)$$

Figure 3.1: Example of the cross section (in cm^2 or Barn which is equivalent to $10^{-24} cm^2$) for a scattering subprocess ab→n at a hadron collider: the cross section can be decomposed in the sum of integrals over subprocess cross sections sigma and parton distribution functions, the so-called "factorization integral"

3.3 *n*-Tuple file: the Data structure

For the purpose of analyzing events in the most convenient way, we saved collections of phase-space configurations along with additional information and each phase space configuration represent one event[15]. This storing and compressing process has been made using ROOT[1], previously assisted and oriented by a Graph Neural Network in terms of filtering out charged π's, through its routines and storing systems: each event is composed by 3 π tracks (not necessarily with a total charge sum equals to ± 1), a μ track, a reconstructed τ track and a reconstructed B_s track. For each track, many features has been stored: P_t, η, ϕ, mass, charge, the vertex coordinates and other information, retained in a ROOT file as histograms which can be used to cross-check analyses. The Monte Carlo sample contains 2863 events, while the BPHParking Dataset has much higher statistics, with more than 2 million events. For each event we have a vector filled with the most promising candidates selected by the DNN: we can go from 1 candidate per event to hundred of candidates per event.

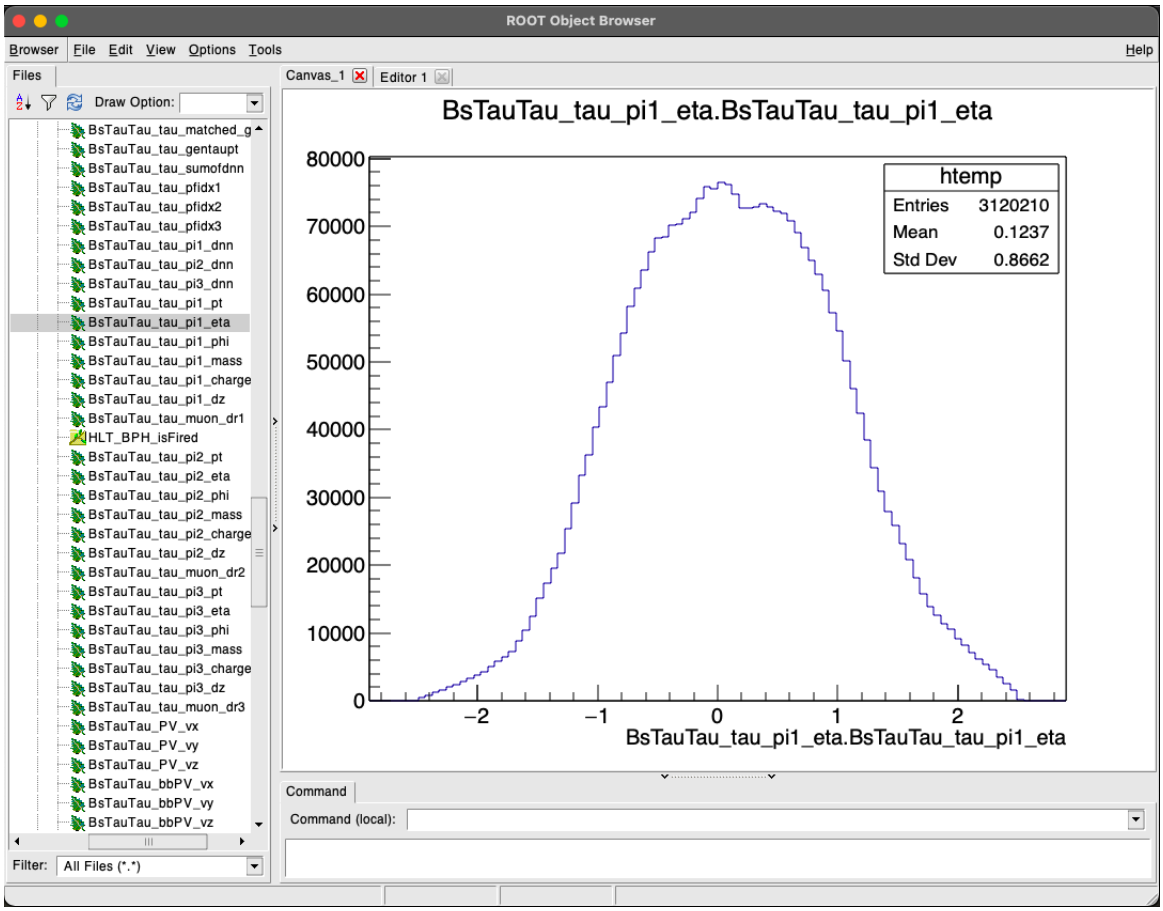

Figure 3.2: BPHP ROOT file

[1]ROOT is a framework for data processing, born at CERN, at the heart of the research on high-energy physics.

Chapter 4

Kinematics of selected events

4.1 Tracks Angles

Considering the great amount of unstable particles that a collision between two highly energetic protons can generate, an helpful classical particle feature is the direction, in the three dimensional space of decayed particles momenta. The momentum of a non relativistic particle is the product of the mass and velocity $\vec{p} = m \cdot \vec{v} = (p_x, p_y, p_z)$, while for a relativistic one we have to take into account special relativity and use the correct formula, considering non-negligible the particle mass $\vec{pc} = \sqrt{\vec{E}^2 - m^2c^4}$. In spherical coordinates centered on collision point, the momentum representation is:

$$\vec{p} = (|p|, \theta, \phi) \tag{4.1}$$

with θ the angle between the particle and the protons beam in verse, and ϕ as azimuthal angle in xy plane, with x headed to the accelerator center and y in vertical direction. Since most detectors are cylindrical, as CMS, the spherical coordinates |p| and θ result quite unusual, so that are replaced with two new parameters: the *Transverse Momentum* $P_t = |\vec{p}| \sin(\theta)$, and *Pseudorapidity* $\eta = -\ln[\tan(\frac{\theta}{2})]$. Hence, in hadron collider physics, linear momentum is represented by

$$\vec{p} = (P_t, \eta, \phi) \tag{4.2}$$

4.1.1 Transverse momentum P_t

The transverse momentum has a key role in HEP: it is, at first order, unaffected from parton distribution functions, which are functions that give the probability to find partons (quarks and gluons) in a hadron as a function of the fraction **x** of the proton's momentum carried by the

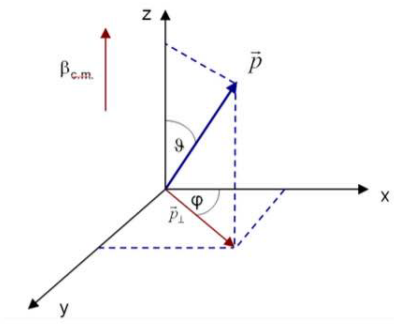

Figure 4.1: P_t representation

parton, therefore P_t gives a scale of how strongly the particle has been emitted from collision. Moreover, under a relativistic point of view, it is a Lorentz invariant feature: consider a particle four-momentum in the Lab system, and assume it is directed parallel to the *z axis*, so that the Lorentz boost is in this axis:

$$\begin{pmatrix} E \\ p_x \\ p_y \\ p_z \end{pmatrix} = \begin{pmatrix} E \\ |\vec{p}|\sin\theta\cos\phi \\ |\vec{p}|\sin\theta\sin\phi \\ |\vec{p}|\cos\theta \end{pmatrix} = \begin{pmatrix} \gamma & 0 & 0 & \beta\gamma \\ 0 & 1 & 0 & 0 \\ 0 & 0 & 1 & 0 \\ \beta\gamma & 0 & 0 & \gamma \end{pmatrix} \cdot \begin{pmatrix} E^* \\ |\vec{p}^*|\sin\theta^*\cos\phi^* \\ |\vec{p}^*|\sin\theta^*\sin\phi^* \\ |\vec{p}^*|\cos\theta^* \end{pmatrix}$$

Figure 4.2: Squaring both sides of the x and y components, and summing these two we have $|\vec{p}|^2\sin^2\theta\left(\cos^2\phi+\sin^2\phi\right) = |\vec{p}^*|^2\sin^2\theta^*\left(\cos^2\phi^*+\sin^2\phi^*\right)$ from which we can conclude $p_t = |\vec{p}|\sin\theta = |\vec{p}^*|\sin\theta^* = p_t^*$.

Since protons that collide head on have identical values of momentum of $7\ TeV/c$ and are practically opposite in direction, the total sum of all particles momenta must be null. A similar path can be done involving transverse momentum in itself: theoretically all momenta sum must be 0, however, in practice this requirement is of no experimental use, because proton remnants and other particles with soft transverse momentum components escape unobserved along the beam line. We can, however, rely on the sum of transverse momenta (of all particles, both charged and neutral, that have been detected) to infer the presence of non-interacting particles, such as neutrinos.
As described in Chapter 3, we have several events, with possibly more than one *Tau Hadronic Candidates*, and for each candidate we have three pions and one muon tracks. Due to the isotropy of space, particles are emitted in every direction of the transverse plane, making the identification of similar events, or rather, events with similar azimuthal distances between the three pions P_t and muon P_t an hard work, also for a Deep Neural Network.
A useful approach to simplify the NN task is to operate a dimensionality reduction by leveraging the symmetries of the system. In order to do that, we have to choose a leading particle, in respect of which can be calculated the azimuthal angle difference of the other three. Knowing the event nature, the most reasonable choice is to choose as leading particle the μ track: aligning this track to the *x axis* allow us to set an equal orientation for every candidate.
At this point, the three tracks combinations and their nature must be analyzed: assuming a negative charge of the μ, we have, for a correct candidate, 2 positive π^+ (π_2), and a negative π^- (π_1), and viceversa for μ^+. If we call the azimuthal angle between μ and the only π with the same charge of μ as A_1, it can be expressed with the formula:

$$A_1 = \pi - ||\varphi_\pi - \varphi_\mu| - \pi| \tag{4.3}$$

It correctly defines an angle in $[0,\pi]$ regardless of the sign of the ϕ angles of μ and π, in the plane these two create. In that way, all decays are structured so that the μ define the new x *axis*, and the same charged π is forced to be in first or second quadrant.
The remaining two π with opposite charges with respect to the μ, have to be re-oriented to maintain the same structure as the original one, and in order to do that, the same formula 4.3 can be used with two additional factors, obtaining:

$$A_2 = \pi - ||\varphi_{\pi_1} - \varphi_\mu| - \pi| \cdot \mathrm{sgn}(\varphi_{\pi_1} - \varphi_\mu) \cdot \mathrm{sgn}(\varphi_{\pi_2} - \varphi_\mu) \tag{4.4}$$

where $\mathrm{sgn}(\varphi_{\pi_1}-\varphi_\mu)$ and $\mathrm{sgn}(\varphi_{\pi_2}-\varphi_\mu)$ have the role to conserve the original structure in space of the decay, because formula 4.3 returns the smallest positive angle between two vectors, forcing them to be on positive semi-plane of the y *axis*, losing the original kinematics information.

4.1.2 Pseudorapidity η

In experimental particle physics, pseudorapidity η, is a commonly used spatial coordinate describing the angle of a particle relative to the beam axis. It is defined as

$$\eta = -\ln\left[\tan\left(\frac{\theta}{2}\right)\right] \tag{4.5}$$

where θ is the angle between the particle three-momentum $\vec{p}$ and the positive direction of the beam axis. In hadron collider physics, the rapidity (or pseudorapidity) is preferred over the polar angle θ because particle production is constant as a function of rapidity, and because differences in rapidity are Lorentz invariant under boosts along the longitudinal axis. This is an important feature for collider physics, where the colliding particle carry different longitudinal momentum fractions, which means that the rest frames of the particle-particle collisions will have different longitudinal boosts.

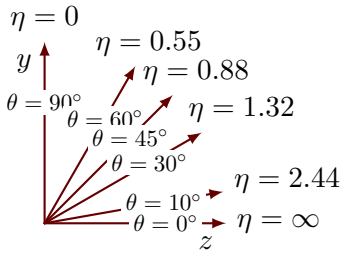

Figure 4.3: As θ approaches to 0, η tends toward ∞

The candidates this analysis is searching for have a strong characteristic in η space: the difference in η between particles involved in these decays must be around 0, in order to have compact regions in space, such as a cone, where particles are close each other.

4.2 Missing Transverse Energy

Neutrinos are neutral, weakly interacting particles, and they escape from typical collider detectors without producing any direct effect in the detector elements. The presence of such particles must be inferred from the imbalance of total momentum. The vector momentum imbalance in the plane perpendicular to the beam direction, the so called transverse plane, is particularly useful in pp and $p\bar{p}$ colliders, and it is called missing transverse momentum, here noted with $\overrightarrow{\mathbb{E}}_{\mathrm{T}}$, and its magnitude is known as missing transverse energy, $\mathbb{E}_{\mathrm{T}}$. A spurious nonzero $\mathbb{E}_{\mathrm{T}}$ in an event can depend from many sources, including measurement resolution, reconstruction inefficiencies, instrumental defects, and improper pattern recognition. Events in which the reconstructed $\mathbb{E}_{\mathrm{T}}$ is consistent with contributions solely from particle measurement resolutions and efficiencies can be identified constructing various features, relating the magnitude of the $\mathbb{E}_{\mathrm{T}}$ with the angle its vector representation $\overrightarrow{\mathbb{E}}_{\mathrm{T}}$ forms with μ three-momentum, for each event, here named *MET-significance*:

$$\mathbb{S} = \frac{Angle(\phi_{\mathbb{E}_{\mathrm{T}}}, \phi_{\mu})}{\sqrt{\mathbb{E}_{\mathrm{T-sum}}}} \tag{4.6}$$

where *Angle* is referred to formula 4.3 with $\phi_{\mathbb{E}_{\mathrm{T}}}$ and ϕ_{μ} as parameters, and $\mathbb{E}_{\mathrm{T-sum}}$ is the total amount of missing transverse energy per event.

4.3 Masses of Resonances

Most of the actually known particles are unstable, and their lifetimes and masses is strongly linked to resonance process. This procedure is divided in two main categories: *resonance in*

formation and *resonance in production.*

4.3.1 Resonance in formation

The cross section σ, which is a measure of the probability of the interaction, is expressed in terms of **s**, Mandelstam variable which corresponds to the center of mass energy, Γ the energy width of the state, and **M** rest mass of the particle concerned, expressed by the Breit-Wigner distribution:

$$\sigma(\sqrt{s}) = \frac{d\ \mathrm{N}}{d\sqrt{s}} \propto \frac{s\Gamma^2}{(s - M^2)^2 + s\Gamma^2} \tag{4.7}$$

When **s** approaches to **M**, σ increases, modulated by the relative value of Γ. Therefore, with an energy scan from low to high ranges of energy, at high numbers of counts corresponds a formation of a particle at rest.

4.3.2 Resonance in production

Final state particles might come from a particle resonance decay, which has a short lifetime which makes the particle undetectable directly. In fact current detectors are able to observe objects with a track length $L = \beta\gamma c\tau$ larger than approximately 1 meter. This is due to the mean lifetime τ, which is inversely proportional to the state energy width Γ coming from the B-W distribution (eq. 4.7). Hence, a peak can be reconstructed computing the invariant mass of the mother-particle, using the daughters features as momenta and masses, thanks to:

$$M = \sqrt{\Sigma_i E_i^2 - (\Sigma \vec{p}_i)^2} \tag{4.8}$$

4.4 Data Analysis

The Monte Carlo sample and B Physics Parking data set n-Tuple have basic information about the decay: as previously written in Chapter 3, each event contains one more candidates, and each candidate holds a triplet of π, a μ, a missing transverse energy vector and a reconstructed τ and B_s, together with other higher level information. Due to the total charge conservation through the decay chain, final products charge sum must be 0, so that if we have a μ^-, in a correct decay candidate we must have $\pi^+\pi^-\pi^+$ coming from the other τ involved, and viceversa for a μ^+. Therefore, the first simple tool that could be useful to a DNN is giving a score to each event, based on the number of correct charge matching candidates per event: calling N_c the number of correct charge matching candidates per event and N_{tot} the number of candidates of the event, we can obtain a good scoring formula as $S = \frac{N_c}{1+N_{tot}}$, so that where we have one candidate per event with correct matching charges the score is $S = \frac{1}{2}$, and where there are no good candidates S is 0. For all other possible combinations, S is included in $[0, 1[$.

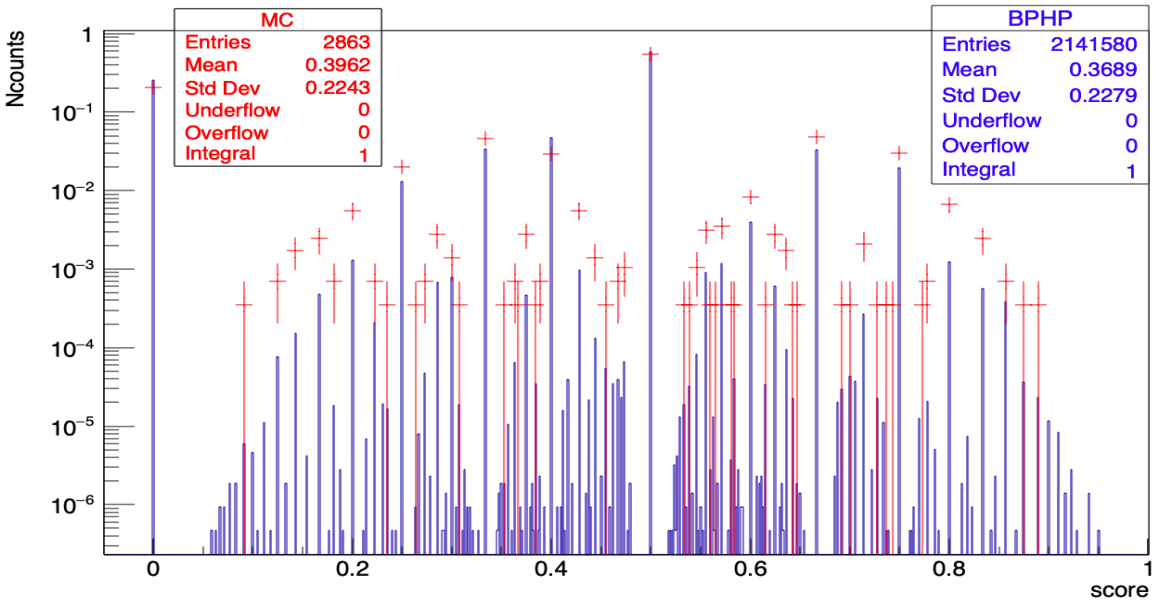

Figure 4.4: S score for both sets: MC(red) and BPHP(blue). Log scale on Y-axis.

A raw division, based on the S score and designed to group together candidates that could come from the searched B_s decay, has been done creating 4 sets for each Dataset(MC and BPHP):

- Set 1: only one candidate per event, with the correct matching charge sum
- Set 2: more than one candidate per event, with at least one candidate with the correct matching charge sum
- Set 3: only one candidate per event, with the wrong matching charge sum(could be $\pm$ 1)
- Set 4: more than one candidate per event, with at all candidates with wrong matching charge sum(could be $\pm$ 1)

Set 1 represents, with high probability, the most promising group of Tau hadron candidates, followed by *Set 2*, where we have correct candidates in terms of total charges, alongside with wrong matching charges candidates. *Set 3* and *Set 4* are useful samples to evaluate the background and the behaviour of the wrong candidates, helping to estimate if some effects are due to noise fluctuations or hide other phenomena.
Furthermore, considering the kinematics of the process, particles must be emitted close each others: we have additional discriminant high level features to be taken into account, in order to improve the quality of candidate choices. Using the Monte Carlo dataset as a model of searched event, we can extrapolate data cuts which optimize the dimension of the sub-sets we are creating and also direct our analysis towards the most interesting candidate: in fact, avoiding the gen-matching routine, the n-Tuple contains boolean variables, which are true under specific requirements, that indicate if candidate have a high probability of being the searched decay. Hence, the next step is find a sort of thresholds, in terms of $Angle_1$(4.3), $Angle_2$(4.4) and $\Delta\eta$ between μ and three π, thanks to which the percentage of the remained events after that cut is 95% or larger. The 6 found thresholds are:

- $A_1 < 1.5$ radiant, for same μ-charged π
- $|A_2| < 1.5$ radiant, for the first opposite μ-charged π
- $|A_2| < 1.5$ radiant, for the second opposite μ-charged π
- $|\Delta\eta| < 2$ for same μ-charged π
- $|\Delta\eta| < 2$ for the first opposite μ-charged π

- $|\Delta\eta| < 2$ for the second opposite μ-charged π

After these cuts, each Set is divided in two *Sub-sets*:

- "Good" Sub-set: candidates suits all cut's criteria
- "Bad" Sub-set: candidates fail one or more criteria

This analysis is mainly focus on *Set 1* and *Set 2*, and in their relative *"Good" Sub-sets*, using *Set 3* and *Set 4*, and *"Bad" Sub-sets* as different types of background/noise samples.

4.4.1 Transverse Plane

Starting from *Sets 1 and 2*, by construction of the *"Good" sub-sets*, all angles of this last sets are smaller than 1.5 radiant for the variable A_1, but we can see that, shifting from *"Good" sub-sets* of *Sets 3 and 4*, tails become larger. Considering variable A_2, for the same previous reason, its magnitude is smaller than 1.5 radiant, but in *Set 1* the distribution is almost symmetric with its mean at 0.179, while the others, coming from *Set 2-3-4*, tend to have a predominant tail at positive values. This fact is due to the construction of the new orientation in space of π_1, which has always positive angles with respect of the μ, and since Pions are emitted close to each others, more symmetric is the distribution peaked at small values above 0, more likely the candidates we are selecting could be the right candidates.
"Bad" sub-sets reveal that in candidates which do not suits all criteria, all π are mainly emitted in the opposite direction to the μ of the event.

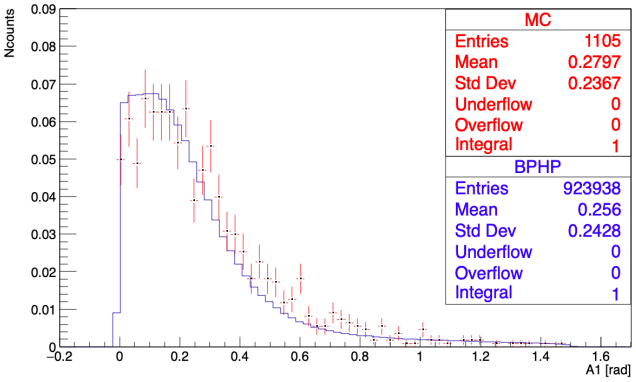

(a) Angle 1, 1°Set, Good sub-set

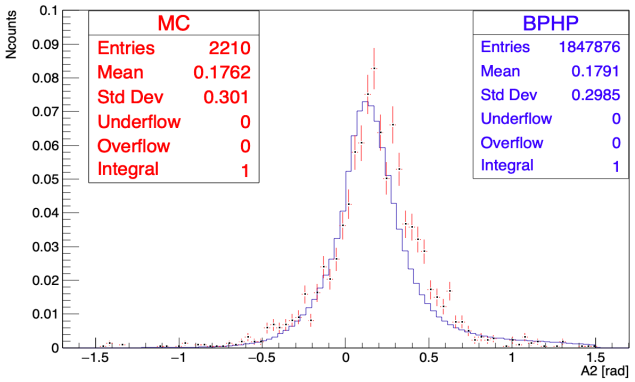

(b) Angle 2, 1°Set, Good sub-set, $4 < P_t < 7$ Gev

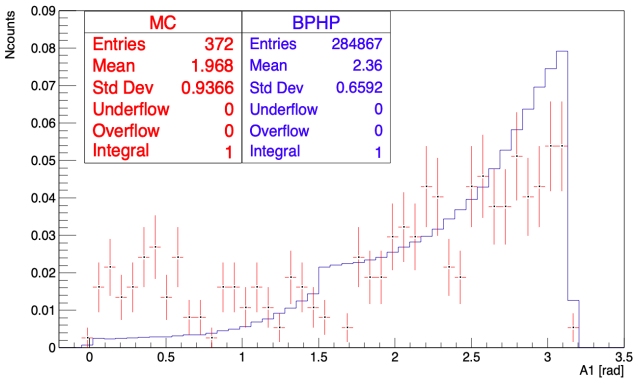

(c) Angle 1, 1°Set, Bad sub-set

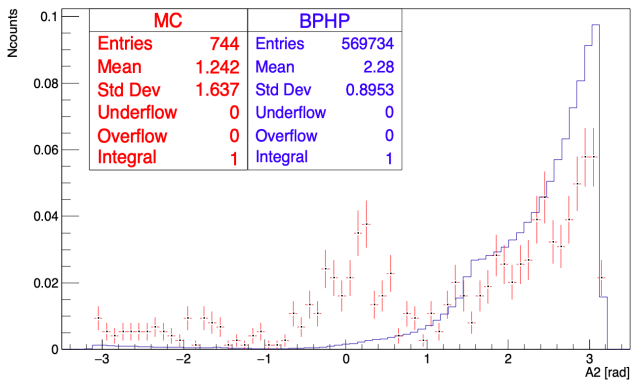

(d) Angle 2, 1°Set, Bad sub-set

Figure 4.5: Transverse plane angles between μ and π's

4.4.2 Eta

We identified, in the previous section, π tracks whose projections in the transverse plane are close each others and, most important, to the μ projection. To create a three dimensional reconstruction of the event with a structure un-effected by symmetrical ambiguity, in addition to the angles in the transverse plane, we must analyze η distributions of π's in relation with the η values of the μ, through $\Delta\eta$ between μ and 3π. Considering *"Good" sub-sets*, in which $|\eta|$ is smaller than 2 by construction, *Set 1* has the mean of the distribution very close to 0 and still represent the most promising set, since the pick in $\Delta\eta$ is the narrowest of 4 sets, with a Standard Deviation of $0.35 GeV/c^2(BPHP)$ and $0.3 GeV/c^2(MC)$, while in *Set 2, "Good" sub-set*, the STD deviations reach values of $0.43 GeV/c^2(BPHP)$ and $0.6 GeV/c^2(MC)$, showing how first set contains event with those characteristics we are searching for, namely the closeness in Eta space between μ and 3π. *"Bad" sub-sets* show Gaussian distributions, reaching values from -4 to 4, with large std. deviations, collecting background events.

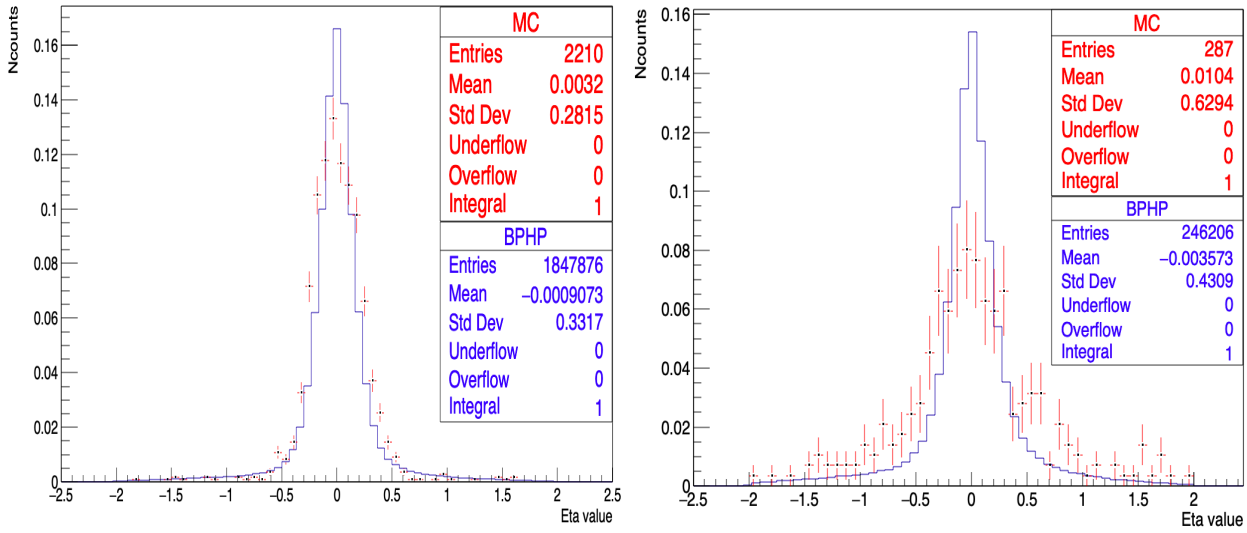

Figure 4.6: Eta distributions, Set 1 (Left) and Set 2 (Right)

4.4.3 Missing Transverse Energy

MET-significance provides a chance to evaluate how neutrinos are arranged in respect of μ: in an high-energy process, to conserve the total four-momentum sum, the kinematics of decays lead $\mathbb{E}_T$ and the Muon to be emitted in two main configurations: *back-to-back* or *aligned in the same direction*. In this analysis, to emphasize this behaviour, four different classes were created, according to missing transverse energy value, and analyzed the MET-significance (4.6) for each of them:

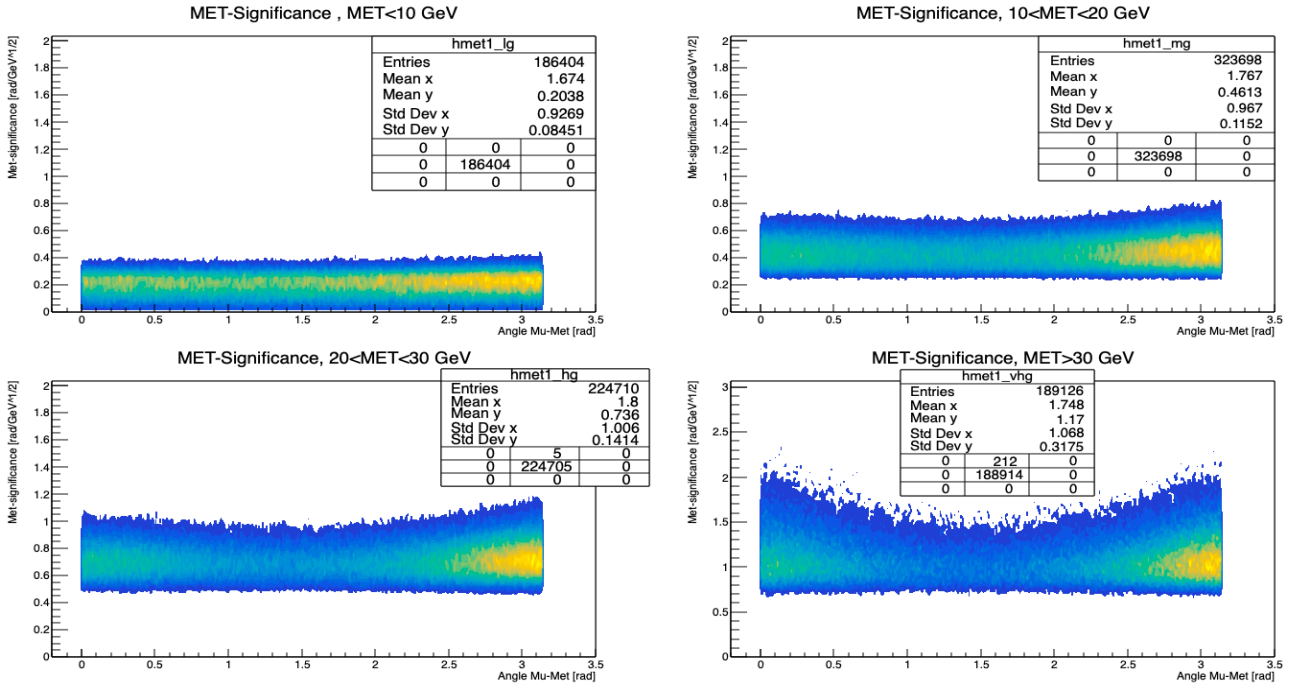

Figure 4.7: Met significance for BPHP

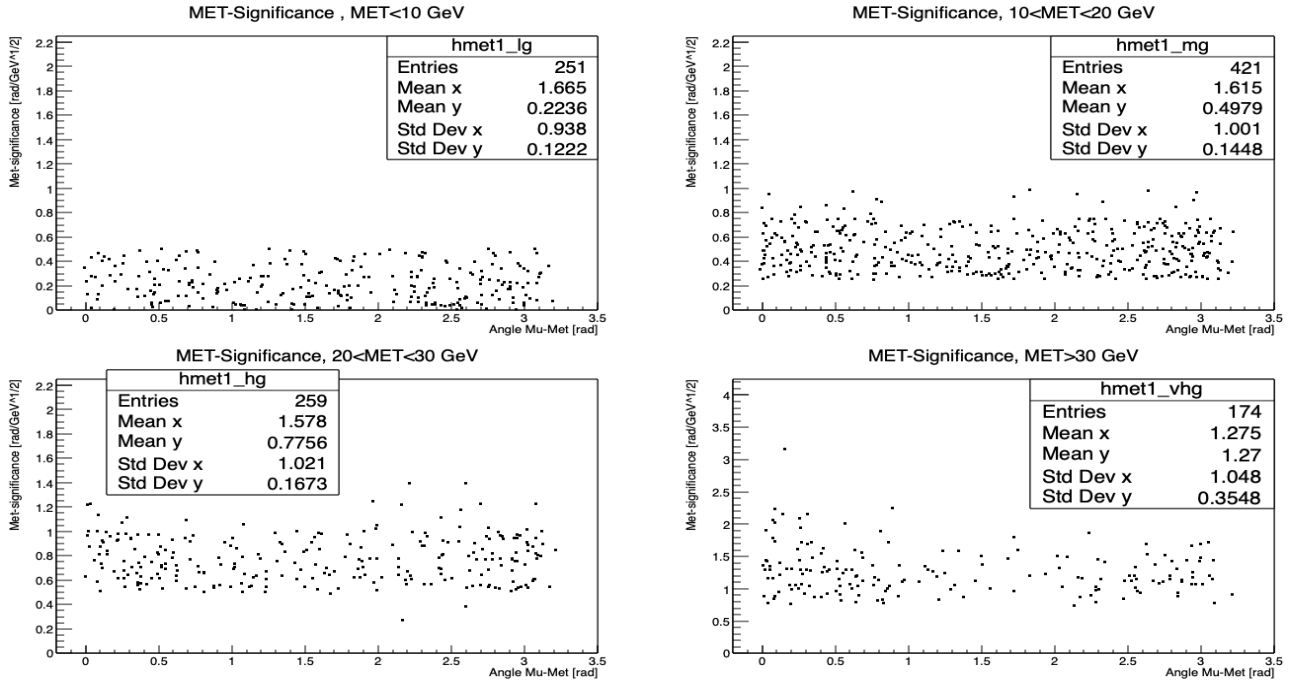

Figure 4.8: Met significance for MC

Starting from low energy values, the distribution is almost flat, with a little higher concentration of events around π, while approaching to high energy values, distributions become concave, with strong concentrations at 0 and π. These observations lead to the conclusion that the $\mathbb{E}_{\mathrm{T}}$ represent a useful tool to roughly visualize neutrino's tracks, helped by *MET-significance*.

4.4.4 Masses

The ρ meson decays in two π, and being the mother-particle neutral, Pions will be π^+ and π^-. Thus, one of the 2 π with opposite charge, compared to the μ, must be chosen to be part of the

ρ products. In order to avoid any kind of losses of information, reconstructing the mass of the meson by the resonance in production technique, we used both combinations of $\pi^+\pi^-$, storing the closer to *776 MeV* for the Neural Network.

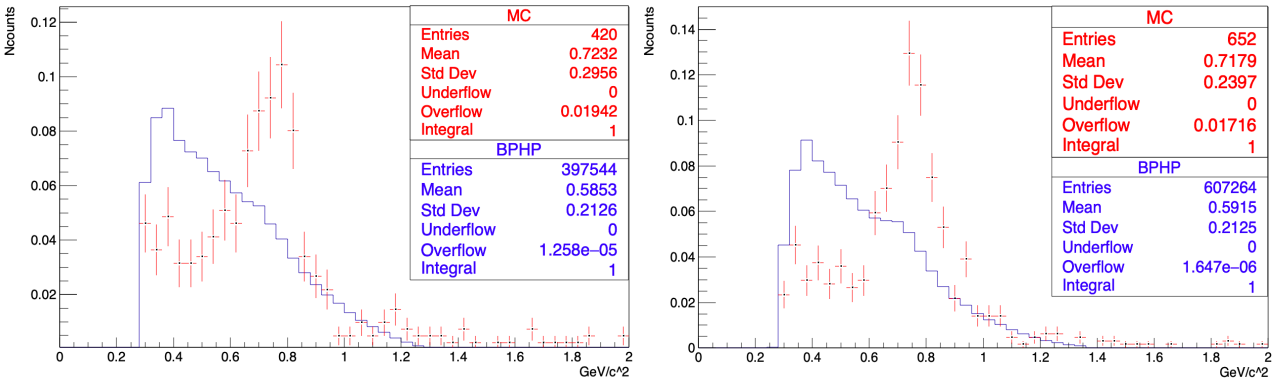

(a) Rho mass, 1°Set, $P_t < 4$ Gev

(b) Rho mass, 1°Set, $4 < P_t < 7$ Gev

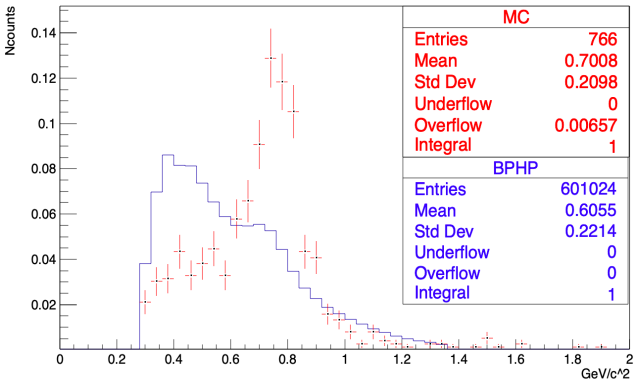

(c) Rho mass, 1°Set, $7 < P_t < 14$ Gev

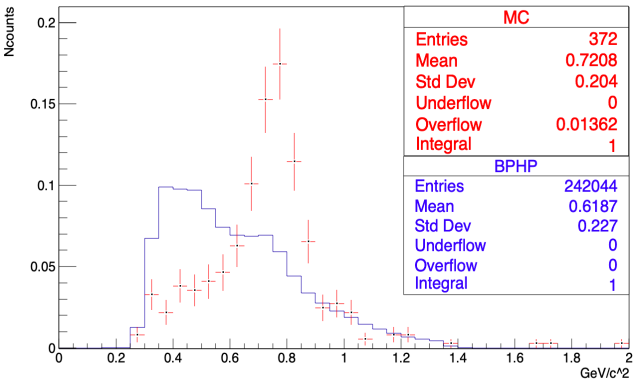

(d) Rho mass, 1°Set, $P_t > 14$ Gev

Figure 4.9: Rho Masses divided by their P_t

The differences in shape between *MC* and *BPHP* datasets is clearly evident: the simulation presents a pointed peak at the ρ mass threshold, with some secondary effects at smaller values. On the contrary, BPHP have an opposite behaviour: the most prominent peak stands at low values, while the ρ cusp is clear only at high P_t values.

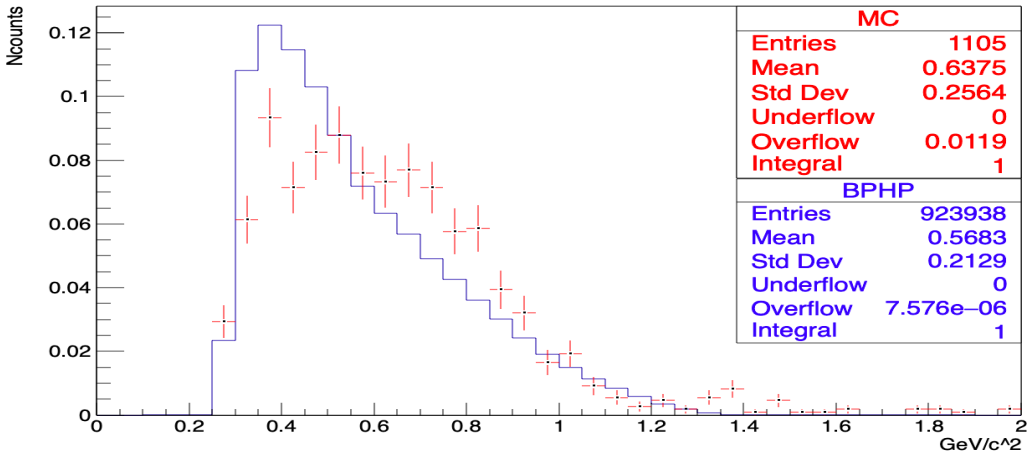

Figure 4.10: Wrong combinations for MC and BPHP

In order to evaluate this low energy peak, we computed the invariant mass using 2 π with same

charges, trying to estimate the noise that a bad pairing, in terms of decay products, could create: results give us some useful information, whereas they provides us a clear cluster of reconstructed masses at low values of energy (both for MC and BPHP), compatible with fig 4.9, and good model to evaluate the envelope of the distributions tails.

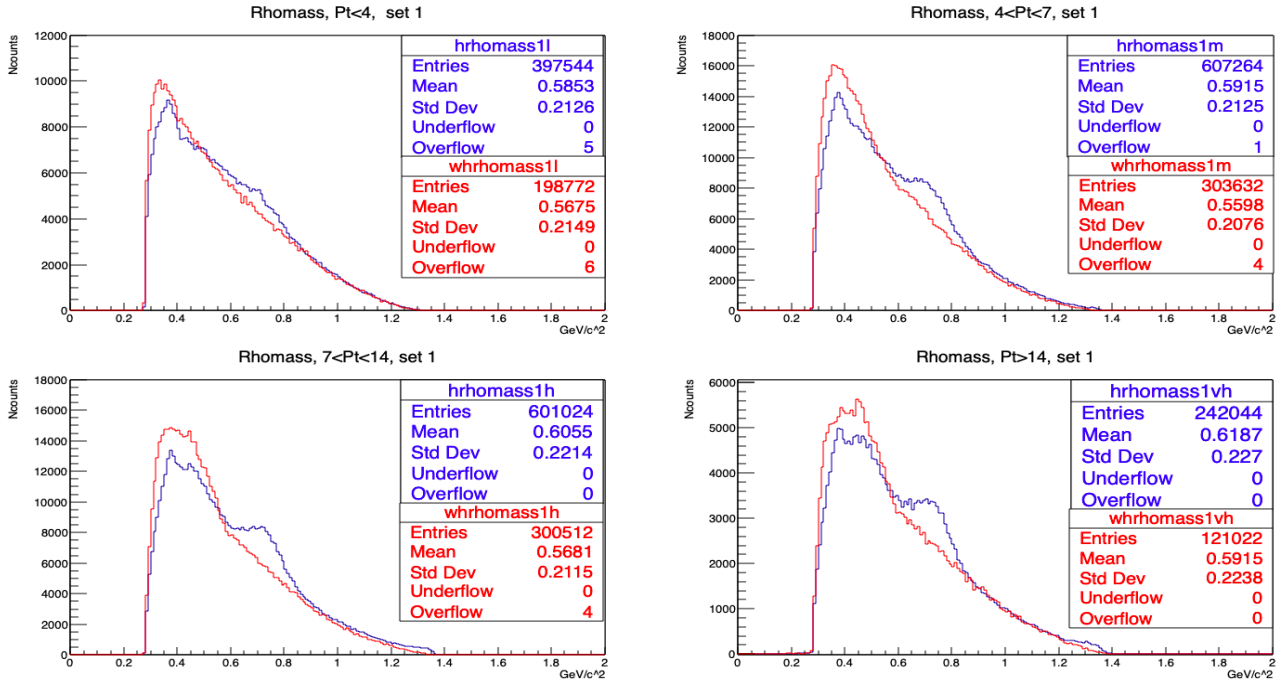

Figure 4.11: Correct Combination(Blue) and Wrong Combination(Red), BPHP

ρ center-of-mass system

An helpful tool to analyze the structure of the ρ decay could be moving into the center of mass system, where the total momentum sum is null: the angles between particle momenta, in this system, can determine if there is a clear structure in the products. As regards the decays we are searching, we have, in the second last step of the chain, a ρ meson, a π and μ such that the total charge sum is 0. So that, if the 2 π decaying from the ρ have some different behaviour on respect of the last Pion, boosting them in the center of mass system could give us important information. First we have to select candidates which have a mass value close to the ρ mass value, to restrict the analysis to an high concentration ρ sub-set: the algorithm select candidates with a mass between 766 and 786 MeV. Once we are boosted-in, to have the same orientation for each event, selecting the π with same charge of the μ, which is the constant particle in both 2 combination and we will call it π_0, we can evaluate the angle in the transverse plane between this and the other π's (α_1 and α_2) composing the ρ, and the other with the single free π:

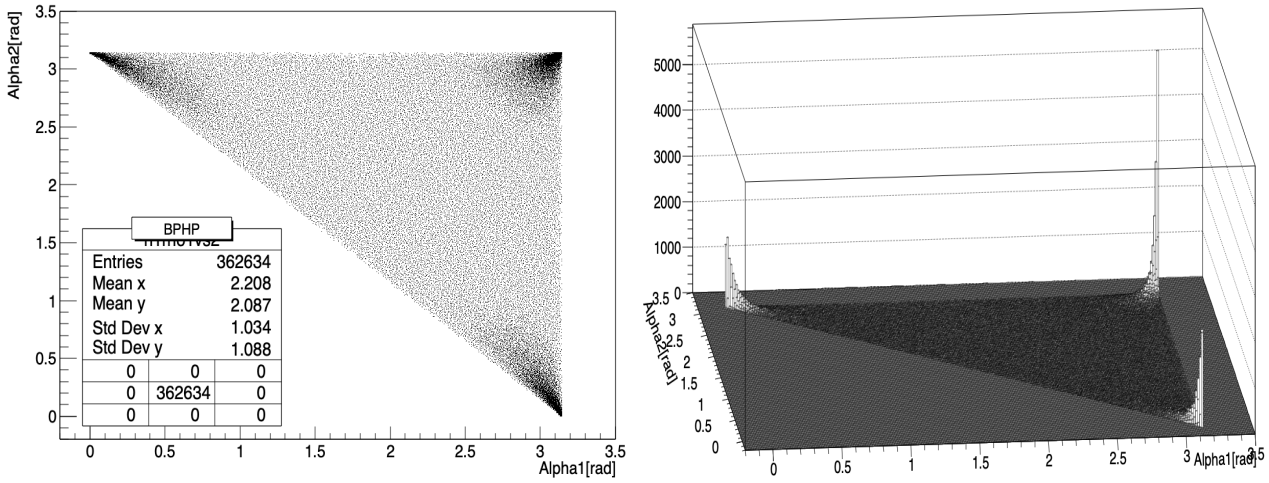

Figure 4.12: α_1 vs α_2 scatter plots

Figure 4.12 shows an evident result: angles, are most of the cases, 0 or π for both particles, consistent with the center of mass kinematics, but without any particular structure. To be more clear and go deeper in the nature of the system, following the total momentum conservation, the configuration with two angles equal to π radiant should be preferred when the momentum of the constant Pion, the one we are taking as *x axis* tends to higher values. So that, plotting in a 3 dimensional space the previous scatter plot in the *y-z plane*, and adding as new dimension in the *x axis* the constant π momentum, it can be checked if the most frequent angular combination in fig.4.12 is due to kinematics laws or not:

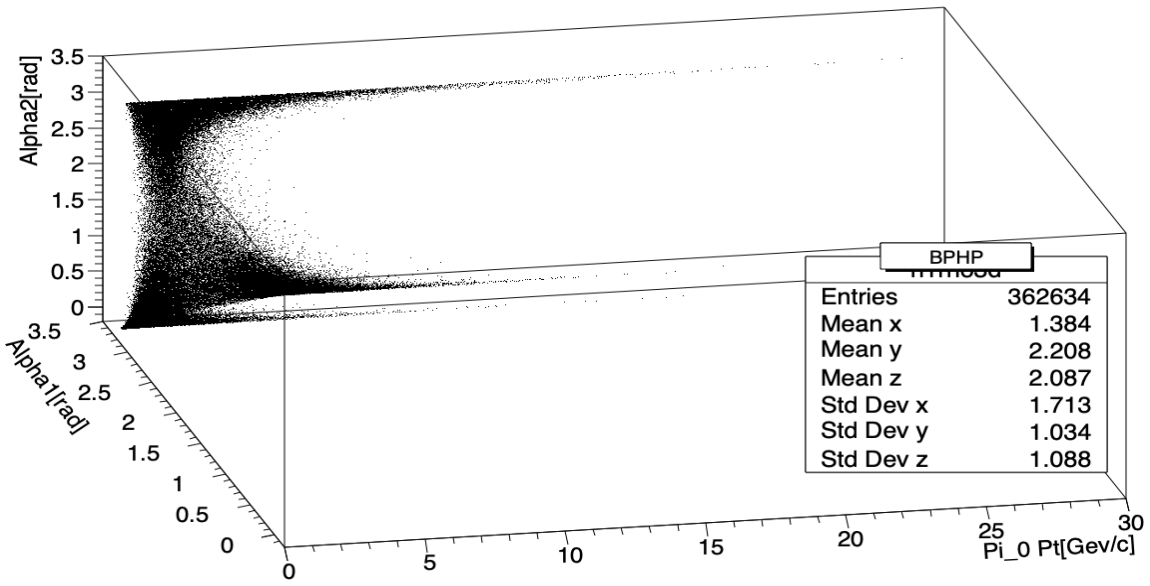

Figure 4.13: Added the P_t of the π_0 in x-axis at the previous scatter plot(in y-z plane)

ϕ and D mesons

Taking into account only the BPHP dataset, which has much higher statistics and has collected various possible candidates, and watching carefully its envelope, there are signs of others possible misinterpreted decays.
Considering that we are dealing with an heavy flavours dataset, one of the most common particles detected in these sets is the ϕ meson, with a mass of *1019 MeV*, which plays the role of a decay product coming from a B or D meson decay chain. Since the main decay of the ϕ meson

is $\phi \to K^+K^-$, with a *branching fraction* $\Gamma_i/\Gamma = 49.2\%$, we tried to assign the mass of the $K^{+/-}$ mesons to the π's, checking if some of the latter ones are, in deep, Kaons decayed from a ϕ. Candidates that fulfill this request should be discard by the DNN, representing background.

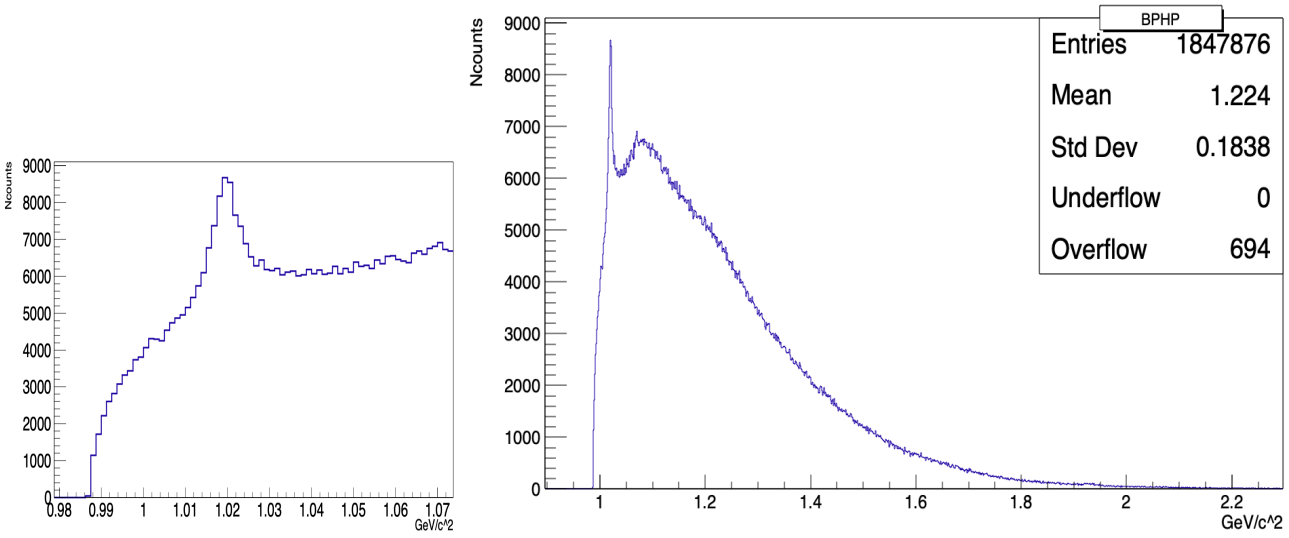

Figure 4.14: ϕ mass reconstruction for BPHP, zoomed around the ϕ mass value(left).

A further, more massive, particle that can be found in this dataset, since it is strongly connected to weak interaction decays and heavy flavours, is the D meson. D mesons are the lightest particles containing charm quarks and, in order to decay, they must change the charm (anti)quark into an (anti)quark of another family. Such process involves a change in the charm quantum number, and can take place only through an exchange of a W particle, changing the charm quark into a strange quark. Therefore, the main products of the D meson decay are K and π. Hence, to verify the presence of this particle, we swapped the mass of one π of the triplet with the mass of the K: we can have many swap combinations given the structure of the triplet, but the most effective is made assigning the K mass to the π with the same charge of the μ.

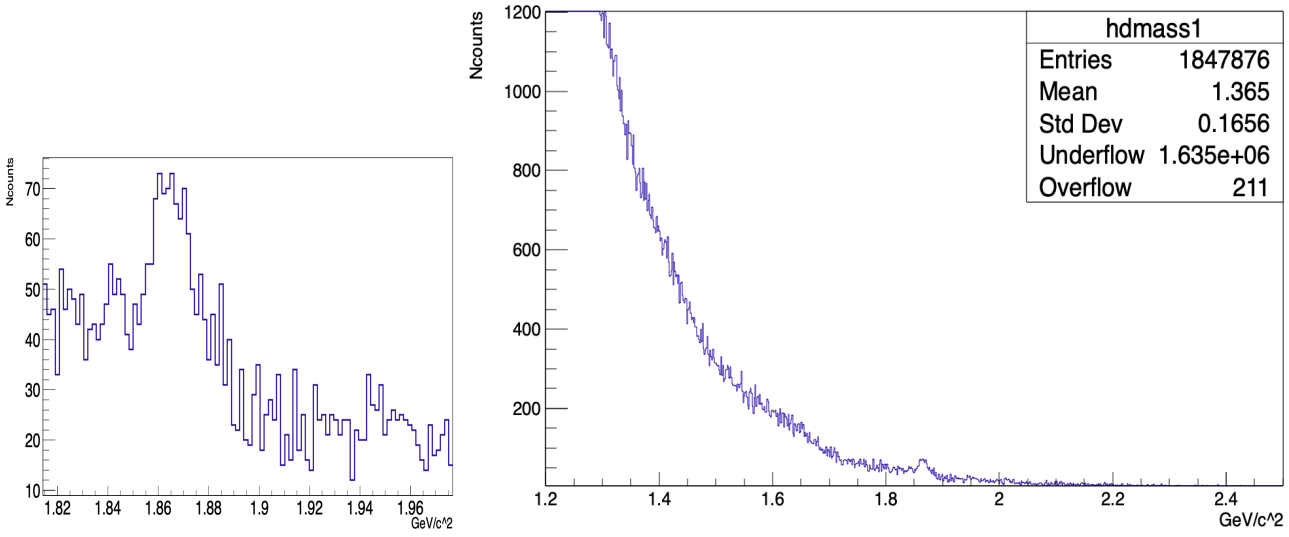

Figure 4.15: D mass reconstruction for BPHP, zoomed around the D mass value(left).

The tail shows a discontinuous fall, interrupted by a peak around 1.86 GeV, that is the D meson mass value, confirming the presence of the meson.

4.4.5 Masses Hypothesis

If ρ and ϕ mesons are clearly reconstructed by previous analysis, there are other particles, belonging and non-belonging to the decay chain, that have an higher complexity level, in terms of mass reconstruction, then the previous ones. This is due to the nature of the dataset (in which events in it were previously checked by a DNN and discarded if do not suit basic criteria needed for the searched decay) and the complexity of a reconstruction based on reconstructed particles (the $a1$ meson is the mother particle of the ρ meson, of which we obtained the kinematic variables from its products, the π's).

Λ baryon

In a p-p collision, loads of new particles are created, including baryons, which are composite subatomic particles which contains a odd number quarks(at least 3).The Λ baryons are a family containing one up quark, one down quark, and a third quark from higher flavour generations. The Λ^0 has, as third quark, the strange quark, and it can be produced in a collision between high-energetic protons: it has a mass of $1115 MeV/c^2$ and it mainly decays into $p\pi^-$ with a branching fraction of 63.9%.
Hence, taking into account that the tracker and the following PID have an error rate, the proton could be mistaken for a π with an high momentum, in order to match the total energy needed. Swapping the mass of the highest momentum π, in cases where the π charge is positive, with the proton mass and computing the invariant mass with this new assignment, we can evaluate if the dataset has been contaminated by the Λ^0. Considering the high concentration of ϕ mesons, without any kind of discrimination, the reconstruction could include an hidden contribution made of the last mesons mentioned. To avoid this effect, we put a threshold on the mass value: computing the invariant mass of the candidate with 2 K mesons, pretending to reconstruct a ϕ, if the mass value is smaller than 1.1 GeV the candidate is discarded from the Λ^0 evaluating process.

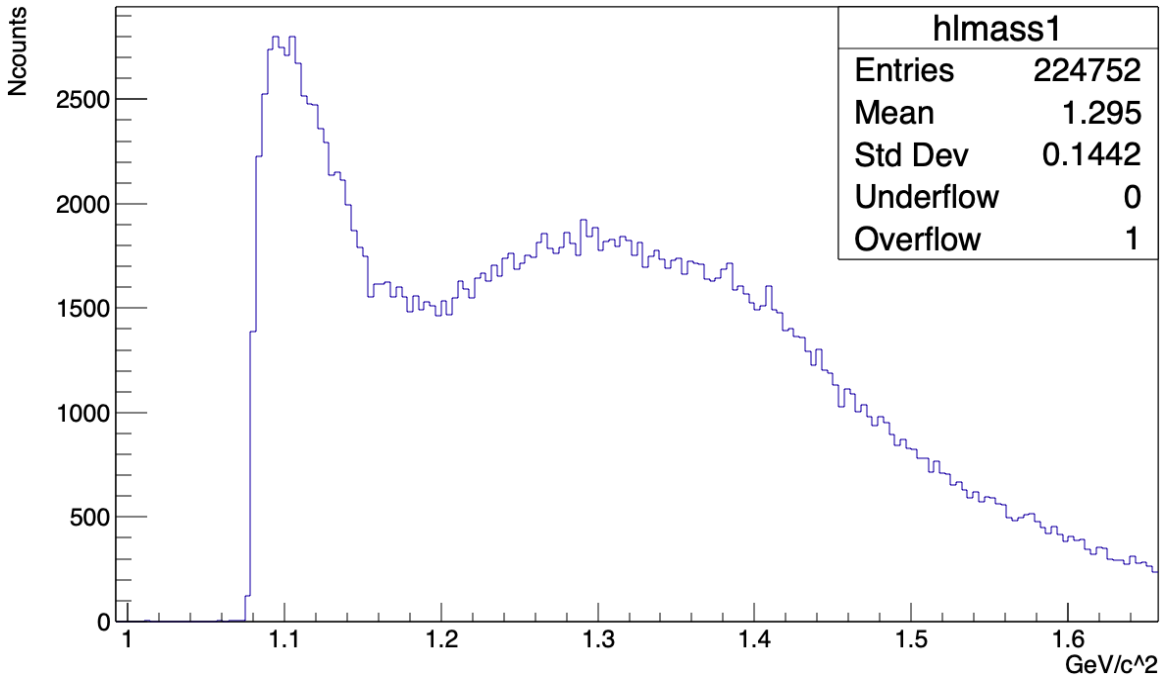

Figure 4.16: Λ^0 baryon reconstruction for BPHP

The plot is essentially showing a clear peak with a mean of 1.1 GeV, with a large width that reduce the accuracy and the confidence of the analysis, because we can not select a single or a

small bunch of bins as the reconstructed Λ signal and have a strong answer to the request of presence of the baryon.

$a1$ meson

The $a1$ meson is the light meson which (in the Wigner classification) is the Lorentz spin group pseudo-vector representation as well as the isospin vector representation, and it is the chiral partner of the ρ meson.[16] With a mass of $(1230 \pm 40)MeV$, this meson mainly decays in a ρ meson and a π. While the kinematic variables of the latter one are available in the *n-Tuple* file, the momentum, the angles and all other variables of the ρ meson must be build from the variables of the π's in which it has decayed. At the end of this job, reconstructing the a1 mass, we should see a pick around 1.2 GeV, with a width from 300 to 600 MeV.

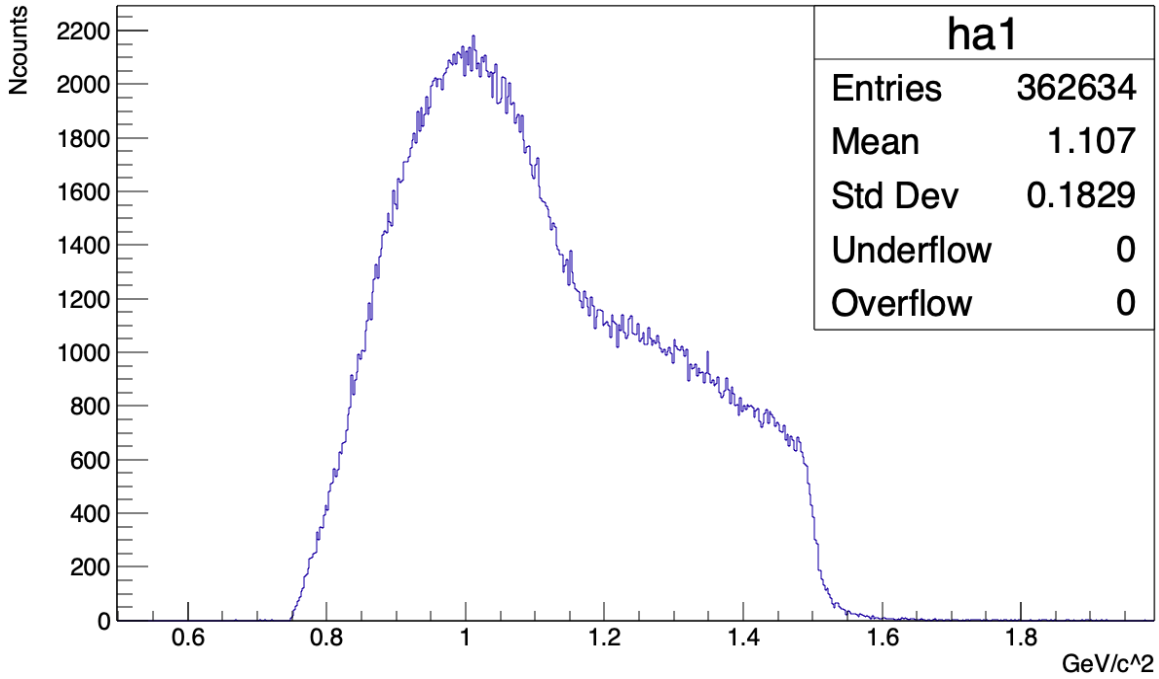

Figure 4.17: $a1$ meson reconstruction for BPHP

If the width seems correspond to the expectation, the mean of the smaller values distributions is quite different from the 1.23 GeV expected: they have their maximum around 1/1.1 GeV, which is close to the a1 mass but not inside the experimental error, which is of a fraction of a percent with tracks of low momentum such as those of our data sample. Hence we can not safely assume the presence of the chiral partner of the ρ meson, but we can suppose that with a clearer ρ signal we could find better results.

Dalitz plots

The Dalitz plot is a two-dimensional representation, mainly used in particle physics, of the relative frequency of different (kinematically distinct) manners in which the products of a three-body decays may move apart. The phase-space of a decay of a pseudoscalar into three spin-0 particles can be completely described using two variables, which are the square of the invariant masses of two pairs of the decay products (i.e. if particle A decays to particles 1, 2, and 3, the Dalitz plot for this decay contains m^2_{1-2} on the x-axis and m^2_{2-3} on the y-axis). If there are no angular correlations between the decay products then the distribution of these variables is flat. Furthermore, three-body decays are often dominated by resonant processes, in which the particle decays into two decay products, with one of those decay products immediately

decaying into two additional decay products. In this case, the Dalitz plot will show a non-uniform distribution, with a peak around the square of mass value of the resonant decay. In this way, the Dalitz plot provides an excellent tool for studying the dynamics of three-body decays.

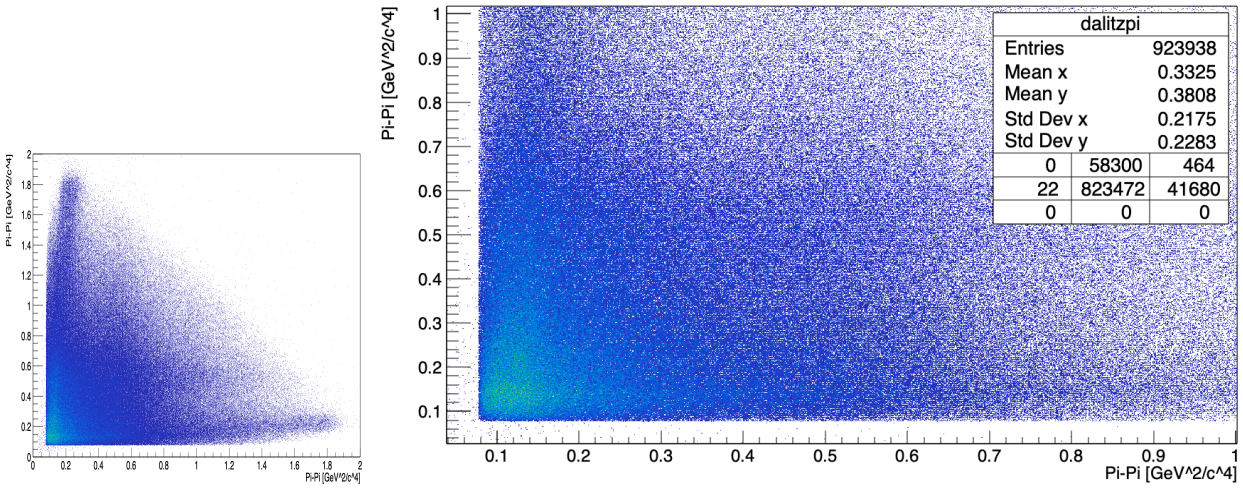

Figure 4.18: ρ Dalitz

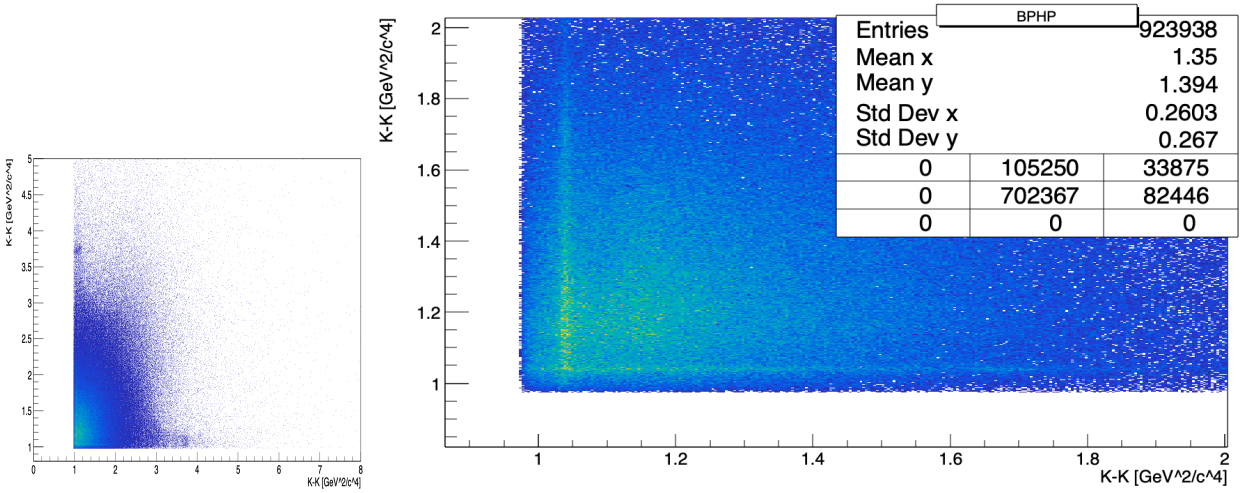

Figure 4.19: ϕ Dalitz

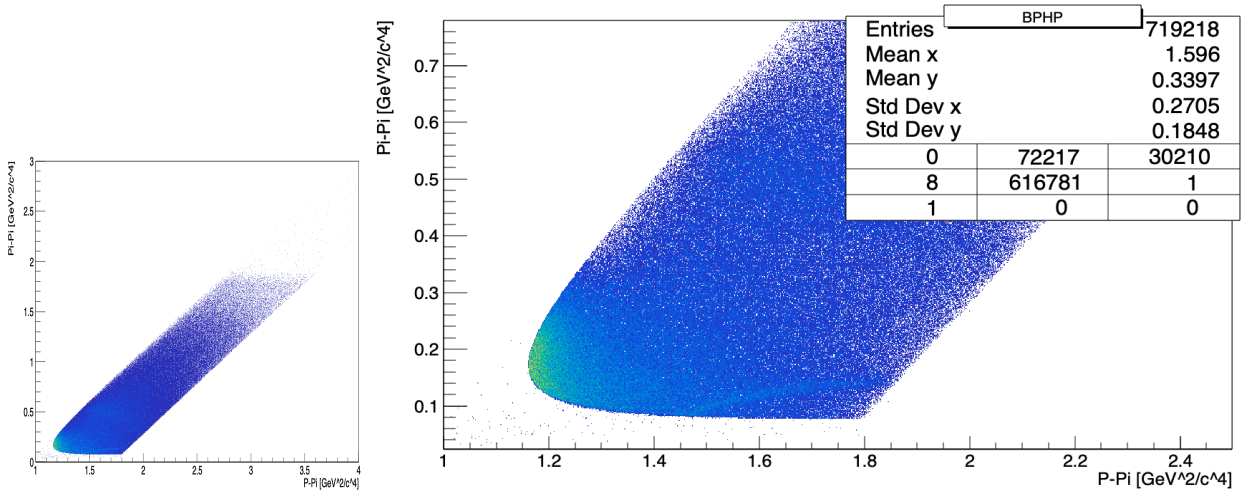

Figure 4.20: ρ/Λ^0 Dalitz

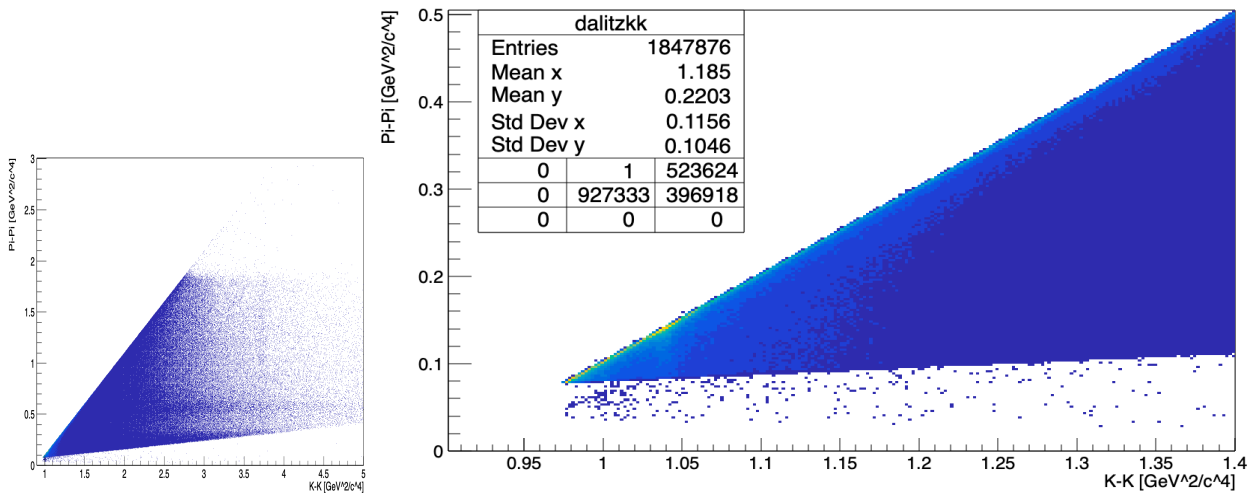

Figure 4.21: ρ/ϕ Dalitz

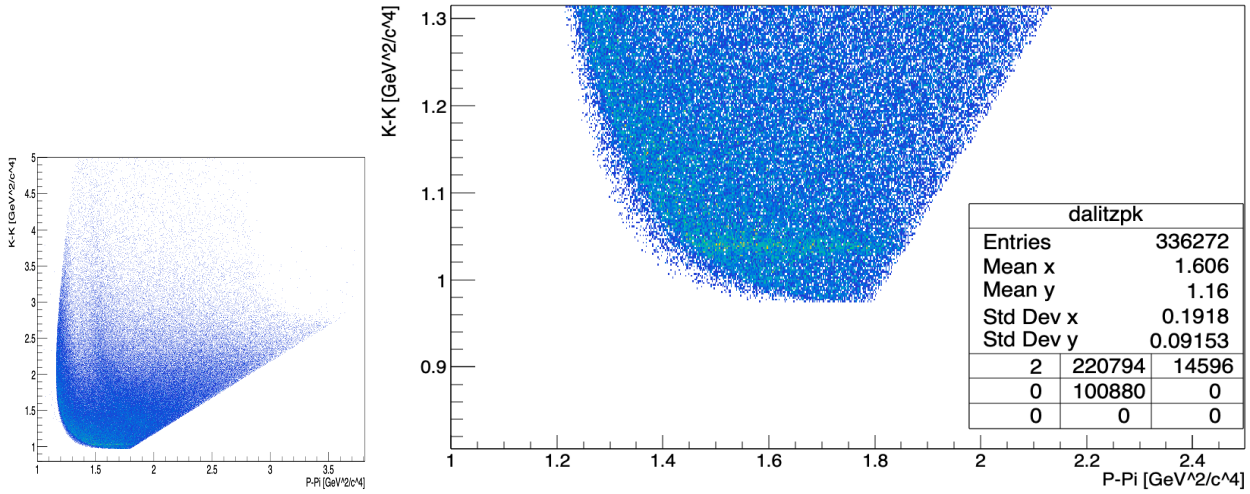

Figure 4.22: ϕ/Λ^0 Dalitz

These scatter plots reveal that the only clear contamination is carried by the ϕ meson, with accumulation stripes in plots 4.22,4.20 and clearly in plot 4.19. Other high density zones, represented in yellow, are mainly threshold accumulations, as in fig 4.20.

Chapter 5

Summary

In this thesis the kinematics of the $B_s \to \tau\tau$ has been analyzed, providing new high level features as the angles in the transverse plane between μ and π's, the $\Delta\eta$ difference between products and particle masses inside and outside the decay chain, aimed to use respectively as signal and background.

Bibliography

[1] *The standard model*. URL: https://home.cern/science/physics/standard-model.

[2] T. Dorigo. *Naturalness explained with the Roulette*. Aug. 2014. URL: https://www.science20.com/quantum_diaries_survivor/naturalness_explained_roulette-94976.

[3] R. Aaij et al. "Search for the Decays $Bs^0 \to$ Tau(+) Tau(-) and $B^0 \to$ Tau(+) Tau(-)". English. In: *Physical Review Letters* 118 (June 2017). ISSN: 0031-9007. DOI: 10.1103/PhysRevLett.118.251802.

[4] D. Bečirević et al. "Leptoquark model to explain the B -physics anomalies, RK and RD". In: *Physical Review D* 94.11 (Dec. 2016). ISSN: 2470-0029. DOI: 10.1103/physrevd.94.115021. URL: http://dx.doi.org/10.1103/PhysRevD.94.115021.

[5] D. Bečirević et al. *Palatable Leptoquark Scenarios for Lepton Flavor Violation in Exclusive $b \to s\ell_1\ell_2$ modes*. Aug. 2019. arXiv: 1608.07583 [hep-ph].

[6] C. Bobeth et al. "$B_{s,d} \to \ell^+\ell^-$ in the Standard Model with Reduced Theoretical Uncertainty". In: *Physical Review Letters* 112.10 (Mar. 2014). ISSN: 1079-7114. DOI: 10.1103/physrevlett.112.101801. URL: http://dx.doi.org/10.1103/PhysRevLett.112.101801.

[7] Pdg. *P.A. Zyla et al. (Particle Data Group), prog. Theor. exp. phys. 2020, 083c01 (2020) and 2021 update*. URL: https://pdglive.lbl.gov/Viewer.action.

[8] B. Aubert et al. "Search for the Rare Decay $B^0 \to \tau^+\tau^-$ atBABAR". In: *Physical Review Letters* 96.24 (June 2006). ISSN: 1079-7114. DOI: 10.1103/physrevlett.96.241802. URL: http://dx.doi.org/10.1103/PhysRevLett.96.241802.

[9] M. Voj'ik, P. Lichard Silesian University in Opava, and Czech Technical University in Prague. "Three-pion decays of the tau lepton, the a_1(1260) properties, and the a_1$\rho\pi$ Lagrangian". In: *arXiv: High Energy Physics - Phenomenology* (June 2010).

[10] *The large hadron collider*. URL: https://home.cern/science/accelerators/large-hadron-collider.

[11] *CMS*. URL: https://home.cern/science/experiments/cms.

[12] *Triggering and Data Acquisition*. URL: https://cms.cern/detector/triggering-and-data-acquisition.

[13] G. Landsberg. *"B Physics parking program at CMS"*. URL: https://indico.cern.ch/event/754760/contributions/3127694/attachments/1714192/2764759/B-parking-RDMS-2018.pdf.

[14] A. Buckley et al. "General-purpose event generators for LHC physics". In: *Physics Reports* 504.5 (July 2011), pp. 145–233. ISSN: 0370-1573. DOI: 10.1016/j.physrep.2011.03.005. URL: http://dx.doi.org/10.1016/j.physrep.2011.03.005.

[15] Z. Bern et al. "Ntuples for NLO events at hadron colliders". In: *Computer Physics Communications* 185.5 (May 2014), pp. 1443–1460. ISSN: 0010-4655. DOI: 10.1016/j.cpc.2014.01.011. URL: http://dx.doi.org/10.1016/j.cpc.2014.01.011.

[16] S. LEUPOLD and M. WAGNER. "CHIRAL PARTNERS IN A CHIRALLY BROKEN WORLD". In: *International Journal of Modern Physics A* 24.02n03 (Jan. 2009), pp. 229–236. ISSN: 1793-656X. DOI: 10.1142/s0217751x09043523. URL: http://dx.doi.org/10.1142/S0217751X09043523.